Hair phenotype diversity across Indriidae lemurs

Running Title: Hair evolution in Indriids

*Elizabeth Tapanes[1I], Rachel L. Jacobs[1], Ian Harryman[1II], Edward E. Louis Jr.[2], Mitchell T. Irwin[3], Jason M. Kamilar[4,5], Brenda J. Bradley[1]

[1] Center for the Advanced Study of Human Paleobiology, Department of Anthropology, The George Washington University

[2] Conservation Genetics Department, Omaha's Henry Doorly Zoo and Aquarium

[3] Department of Anthropology, Northern Illinois University

[4] Department of Anthropology, University of Massachusetts Amherst

[5] Graduate Program in Organismic and Evolutionary Biology, University of Massachusetts Amherst

*= Corresponding author:

Elizabeth.tapanes@gmail.com

[I] Present address of Elizabeth Tapanes: University of California San Diego, Department of Biological Sciences

[II] Present address of Ian Harryman: Stanford University, Department of Earth System Science

Abstract

Objectives

Hair (i.e., pelage/fur) is a salient feature of primate (including human) diversity and evolution—serving functions tied to thermoregulation, protection, camouflage, and signaling—but wild primate pelage evolution remains relatively understudied. Specifically, assessing multiple hypotheses across distinct phylogenetic scales is essential but is rarely conducted. We examine whole body hair color and density variation across Indriidae (*Avahi*, *Indri*, *Propithecus*)—a lineage that, like humans, exhibits vertical posture (i.e., their whole bodies are vertical to the sun).

Materials and Methods

Our analyses consider multiple phylogenetic scales (family-level, genus-level) and hypotheses (e.g., Gloger's rule, the body cooling hypotheses). We obtain hair color and density from museum and/or wild animals, opsin genotypes from wild animals, and climate data from WorldClim. To analyze our data, we use phylogenetic generalized linear mixed models (PGLMM) using Markov chain Monte Carlo algorithms.

Results

Our results show that across the Indriidae family, darker hair is typical in wetter regions. However, within *Propithecus*, dark black hair is common in colder forest regions. Results also show pelage redness increases in populations exhibiting enhanced color vision. Lastly, we find follicle density on the crown and limbs increases in dry and open environments.

Discussion

This study highlights how different selective pressures across distinct phylogenetic scales have likely acted on primate hair evolution. Specifically, our data across *Propithecus* may implicate thermoregulation and is the first empirical evidence of Bogert's rule in mammals. Our study also provides rare empirical evidence supporting an early hypothesis on hominin hair evolution.

Keywords: lemurs, coloration, opsins, integument, adaptation

Introduction

Hair (i.e., pelage, fur) is a salient feature of primate diversity and evolution and is the product of natural and sexual selection. Hair has been found to play a role in conspecific signaling (Allen & Higham, 2013), thermoregulation (Fratto & Davis, 2011), camouflage (Barrett et al., 2019; Hoekstra et al., 2005) and to possibly provide protection from pathogens/parasites (Paus & Foitzik, 2004). Across all mammals, primates—including humans—arguably exhibit the most diversity in hair color (e.g., bright reds) and growth patterns (e.g., mustaches) between and within species (Caro, 2005; Rowe, 1996). For example, within Colobinae, some *Colobus* spp. sport a long black and white dorsal cape, and *Pygathrix* spp. are often tri-colored and short-haired (Rowe, 1996). Similarly, human hair color and texture vary throughout the human body, between individuals, between populations, and can be correlated with ancestry and ethnicity (Lasisi et al., 2016; Seibert & Steggerda, 1999; Steggerda & Seibert, 1941). Nevertheless, our knowledge about hair evolution is based mainly on non-primate mammals. Primate hair remains relatively understudied (with some notable exceptions: (e.g., (Allen & Higham, 2013; Bell et al., 2021; Kamilar et al., 2013; Rakotonirina et al., 2017; Santana et al., 2012)), with most research taking a macro-scale approach and sampling broadly across the primate order (e.g., all catarrhines).

These previous studies indicate that variation in primate hair color likely evolved in response to multiple distinct but not mutually exclusive pressures associated with ecology, visual systems, activity cycles, and sociality (Allen & Higham, 2013; Bell et al., 2021; Kamilar et al., 2013; Rakotonirina et al., 2017; Santana et al., 2012). For example, across primates, melanic (i.e., black) colors often co-occur with humid regions—which may be due to camouflage, pleiotropy, pathogen resistance, or selection on a related trait (i.e., Gloger's rule) (Bell et al.,

2021; Kamilar & Bradley, 2011; Santana et al., 2012; 2013). Gloger's rule generally predicts birds and mammals will be more pigmented in tropical regions where it is warm and humid, such as tropical rainforests (Gloger, 1833). However, without accounting for variation within families, genera, and species, other subtle trends or relationships may not be detected. For example, recent work in birds suggests a distinct rule (Bogert's rule) may explain some melanic variation in endotherms depending on the phylogenetic and geographic scale sampled (Bogert, 1949; Delhey et al., 2019). According to Bogert's rule, melanic colors should co-occur with cold regions as dark colors may absorb heat better and aid in thermoregulation (Bogert, 1949; Delhey et al., 2019). However, there is no current empirical evidence for this rule in primates (or any mammals). Yet across human populations, variation in eumelanin exceeds that seen in red, blonde, or lighter hair (Lasisi et al., 2016), which suggests that important biological variation may be identified if the scale of analyses was smaller than previously considered (i.e., within a few populations vs. across all populations) (Norton et al., 2016).

Across non-human primates, red hues (and facial patterning) may act as a means to aid conspecific communication (Cuthill et al., 2017; Santana et al., 2012; 2013; Winters et al., 2020). For example, diurnal activity and the ability to perceive a wider range of colors compared to other mammals may have contributed to the enhanced color diversity in specific primate clades (Bell et al., 2021). However, the evidence for coevolution of hair coloration, specifically red hair and color vision in primates, remains mixed (Fernandez & Morris, 2007; Kamilar et al., 2013). Our understanding of primate hair color may benefit from broader sampling across wild populations and/or analyses conducted on smaller phylogenetic scales.

Similarly, our understanding of pelage density evolution remains limited to extensive macro-scale studies. Across primates, the primary trend is that hair density decreases as body

size increases (Sandel, 2013; Schwartz & Rosenblum, 1981). One early hypothesis argued that a reduction in body hair density across hominins coupled to increases in activity level, sweat glands, sweat production, and a change to a dry savannah environment may have aided thermoregulation (i.e., "body-cooling hypothesis") (Jablonski & Chaplin, 2000; Post et al., 1975; Wheeler, 1992). Despite various physiological models testing evidence of the body-cooling hypothesis (Chaplin et al., 1994; Schwartz & Rosenblum, 1981; Wheeler, 1992), there is only rare empirical evidence for this phenomenon within primates (Best et al., 2019). There also remains a poor understanding of how hair density in primates may be impacted by other factors, such as climate. Because hair does not preserve in the fossil record, studies on wild primates can provide critical insights into the evolutionary mechanisms underlying one of the most interesting traits among humans.

This study examined whole-body pelage color and hair/follicle density across Indriidae—a diverse clade of lemurs. Since the Indriidae clade varies in critical aspects known to drive primate (including human) hair variation, they make a good proxy for testing multiple hair hypotheses that have not yet been jointly assessed in one study. Our overarching goals were to 1) examine if Indriidae pelage variation varies across distinct phylogenetic scales and 2) determine if multiple, non-exclusive selective pressures can impact the same trait. Specifically, we aimed to jointly assess the impacts of climate, body size, and color vision on hair evolution at distinct phylogenetic scales. Collectively, this family (comprising three genera: nocturnal *Avahi* and diurnal *Indri* and *Propithecus*) inhabits almost every bio-climate of Madagascar (e.g., humid rainforest, temperate forests, open spiny forest, mangroves) (Mittermeier et al., 2010). The hair of the 13 species in our study varies intra- and interspecifically in both color (e.g., melanic, tricolored orange) and growth morphologies (e.g., long silky hairs, short hairs) (King et al., 2014;

Mittermeier et al., 2010; Petter & Peyrieras, 1972; Rakotonirina et al., 2014; Tattersall, 1986). Indriidae also vary in body size (≈1kg (*Avahi*), ≈3-8kg (*Propithecus*), ≈10kg (*Indri*))—and phylogenetic relatedness likely impacts body size evolution (Lehman, 2007). Thus, we specifically (1a\2a) aimed to uncover how climate and body size influences: pelage brightness (i.e., black color), hue (i.e., red color), and hair follicle density across Indriidae and within *Propithecus*. We expected that climate impacts pelage color and density evolution distinctly across different phylogenetic scales. We predicted that body size only impacts hair/follicle density, based on evidence from other primates (Sandel, 2013). Diurnal Indriidae (*Indri* and *Propithecus*) also vary in their color vision. In many species, some females have trichromatic color vision (ability to distinguish reddish and greenish hues), while males and other females are red-green color blind (polymorphic color vision; Jacobs et al., 2017). Although this feature occurs in some other day-active lemurs, Indriidae has been found to exhibit greater genetic variation in color vision across species (Jacobs et al., 2017). Accordingly, we (2b) aimed to understand how this variation in color vision impacts pelage hue in diurnal genera. We predicted that populations with enhanced capacity for trichromatic color vision would have individuals with redder pelage (Sumner & Mollon, 2003). Our results provide critical insight into how multiple variables impact primate hair evolution across scales. Importantly, this family consists solely of vertical clingers and leapers, which means they exhibit upright locomotory posture similar to humans (via bipedal hopping (Schmidt, 2011)). Thus, these results (specifically those on hair density) may provide insight into human hair evolution.

Materials and Methods

Hair morphology and body size data collection

We used hair color and density measurements from museum research skins (N_{Total} = 63; N_{Museum} = 59) and living animals in one wild population (N_{Wild} = 4, *P. diadema* from Tsinjoarivo) (SI 1). Museum samples spanned three museum collections (SI 2). In total, we sampled six *Avahi* populations (Figure 1A), 23 *Propithecus* populations (Figure 1B), and four *Indri* populations (Figure 1C). Our sampling included nocturnal and diurnal genera (Figure 1D) across all significant bioclimatic regions in Madagascar (Figure 1E). Many individuals did not have available age or sex-class data. Hence, we did not test for differences between age classes or sex. Although some preliminary evidence suggests there may be subtle pelage dichromatism, sifakas are unlikely highly sexually dichromatic in terms of coloration. Instead, sifakas exhibit more significant visible variation within sexes (i.e., bimorphism in males) (Lewis & Van Schaik, 2007; Mittermeier et al., 2010; Spriggs, 2017; Tapanes et al., 2018). Measurements of hair from wild sifakas consisted of following the same protocol as museum individuals. We also extracted body length (mm), measured from head to tip of tail, from all individuals as a proxy for body size using Photoshop CC 6. We standardized all measurements using the known length of a ruler in the photos. Wild sifakas were captured for ongoing parallel research using a standard capture protocol established by the Prosimian Biomedical Survey Project (PBSP) Team (used on 750+ lemurs, 16+ sites, and 35+ species since 2000) (Dutton et al., 2003; Irwin et al., 2010). Groups were habituated before capture. The capture team was led by a trained professional, and captures were performed at close range using Pneu-dart 9mm disposable non-barbed darts containing tiletamine/zolazepam (Telazol) for immobilization.

<u>Hair coloration collection</u>

We used color-calibrated photographs of all animals (N = 63 individuals; SI 1) and a Canon EOS Rebel SL1/EOS 100D mounted with a Canon EF-S18-55mm f/3.5-5.6 IS STM lens.

We calibrated each image against a color standard with 24 color squares of known reflectance values. The camera color mode was set to 'faithful.' The camera was calibrated with a grey standard to set a manual white balance. All individuals were photographed against dull backgrounds using the adjacent method (Bergman & Beehner, 2008; Kendal et al., 2013). We followed established protocols for calibrating photos in previous studies for both museum and wild specimens (Stevens et al., 2007; 2009).

We used the Red-Green-Blue (RGB) color model and extracted all RGB values using Photoshop CC 6 across 14 body regions. Due to the high degree of variation across the pelage of the *Propithecus* tail, ventral surface, and dorsal surface, we divided measurements of these regions into three quadrants (lower, mid, and upper) (SI 3). If one of these regions was damaged, we took measurements from the center as the "average." Primate hair occupies a relatively small color space, primarily varying along two axes. The first relates to variation in luminance and exhibits little chromatic variation and is captured by similar red, green, and blue values. Thus, we used RGB averages here as a proxy for 'brightness' in a hair patch to indicate if the hair is white, a shade of grey, or black. The second axis of variation is hue and indicates variation along a red/brown axis and can be captured by a ratio of red to green. The latter is because the green and blue channels are most similar, while the red channel exhibits higher values on average. As the Red-Green ratio increases, hair appears increasingly red (Kamilar et al., 2013). We ran a correlation matrix across color values and removed any that were highly correlated with each other ($r > .90$). This reduced our hair color variables to RGB averages and RG ratios for the (1) crown, (2) cheek, (3) dorsal torso, (4) ventral torso, (5) forelimb, (6) hindlimb, and (7) tail. In total, we collected 882 brightness and 882 hue measurements (63 individuals x 14 sampling regions). Previous work on museum skins indicated no effect of storage time on pelage

173 coloration from 142 museum skins collected over 100 years (1898 and 1998) (Kamilar et al.,
174 2013).
175
176 Hair and follicle density collection
177 We used a protocol that borrows from dermatological methods and instrumentation, which
178 automates hair density measurements (Avram & Rogers, 2009). We used CompareViewHair®
179 software (STR Technologies) tools combined with a specialized hand-held digital light microscope
180 (ProScope HR2©; Bodelin) with a 100x lens. The software included a built-in procedure for
181 calibrating the lens and software before use. The hair of an animal was parted, and the lens was
182 placed on the skin. A light within the microscope illuminated the skin and provided needed light
183 for subsequently photographing the area. We collected microscopy images (detailing transects of
184 hair follicles and shafts) and compiled semi-automated measurements in the laboratory using this
185 system. We examined two hair morphology properties: hair density (shafts/cm^2) and follicle
186 density (infundibula/cm^2).
187 We collected three microscopy photos (replicates) from five body regions (SI 4) of each
188 animal (n = 47 individuals) (SI 1) using the hand-held microscope, adhering to a previously
189 established protocol (Bradley et al., 2014). The method provided a visual transect/plot of follicles
190 (i.e., infundibula) and the number of hair shafts emerging from each. We used the 'density tool'
191 in CompareViewHair® software to estimate the number of infundibula per cm^2 (i.e., follicle
192 density). We marked each follicle strand manually and used that number to estimate the final
193 value in any given region (given the specific magnification). However, this protocol assumed
194 that the entire photograph was visible, which was not always the case. Therefore, in our final
195 measurements for 'follicle density,' we used the value the software provided of density per cm^2
196 and divided it by the visible photo's proportion. Similarly, for our final measurement for 'hair

density,' we used the value the software calculated for density per cm^2 and multiplied it by the average number of hairs emerging from each follicle. In total, we collected 235 hair and 235 follicle density measurements (47 individuals x 5 body regions). Previous work on museum skins shows no effect of storage time on pelage density for skins collected over 100 years (Bradley et al., 2014).

Climatic and phylogenetic data collection

We collected climate and environmental data from 33 sampling locations across Madagascar (Figure 1). Specifically, we extracted data from WorldClim (version 1) that consisted of averages from 1960 to 1990. This likely created some noise in the data given museum data spanned the early 1900s to late 1990s. However, Indriidae lifespans (≈20+ years) and generation times are long (≈3-10 years) (Lawler et al., 2009; Godfrey et al., 2001; Guevara et al. 2018). Thus, the data are likely representative of accurate averages across bioclimates and phenotypes. Localities were obtained from museum records, and we used Google Earth to obtain geographic coordinates of the nearest forested area in the species range. Localities were listed as forests or towns with directional coordinates (e.g., 40 km W of Tamatave). We used R packages 'raster' and 'sp' to extract all localities' climate data in the WorldClim database (Hijmans & Etten, 2012; Pebesma & Bavand, n.d.). We ran a correlation matrix for all 19 bioclimatic variables and removed any highly correlated variables ($r > .80$). In the end, we used five bioclimatic variables in our comparative analysis as predictor variables (SI 5).

DNA extractions for opsin genotypes

We categorized diurnal Indriidae color vision status (e.g., polymorphic color vision,

220 dichromatic – red-green colorblind) based on X-linked opsin genotypes (Jacobs et al., 2017,
221 2019). Our analysis included diurnal Indriidae represented by a subset of species/populations for
222 which pelage data were also available ($N_{species}$ = 7; $N_{populations}$ = 10; SI 6). Opsin genotypes for
223 populations of diademed sifaka (*Propithecus diadema*), Milne-Edwards's sifaka (*Propithecus*
224 *edwardsi*), golden crowned sifaka (*Propithecus tattersalli*), Verreaux's sifaka (*Propithecus*
225 *verreauxi*), and *Indri indri* were previously published (Jacobs et al., 2017). Data for the silky
226 sifaka (*Propithecus candidus*) and Perrier's sifaka (*Propithecus perrieri*) were based on opsin
227 genotypes obtained from five individuals from Anjanaharibe-Sud ($N_{X\ chromosomes}$ = 8) and
228 Analamera ($N_{X\ chromosomes}$ = 8) populations, respectively, following (Jacobs et al., 2019). Briefly,
229 we extracted genomic DNA from blood/tissue samples using phenol-chloroform-isoamyl
230 extraction protocols (Sambrook et al., 1989). We used quantitative PCR (Mic qPCR Cycler, Bio
231 Molecular Systems; Rotor-Gene Q, Qiagen) to amplify exons 3 and 5 of the X-linked opsin gene.
232 Amplification was followed by high-resolution melt analysis (HRMA) (*following* (Jacobs et al.,
233 2016)), and we determined genotypes for each exon based on the observed melt curve shape and
234 temperature compared to positive controls ($N_{Replicates}$ = 2 per exon). To further confirm genotype
235 calls, we Sanger sequenced qPCR amplicons from at least two individuals representing each
236 observed melt curve. All sequences matched scored genotypes based on melt curves.
237 We estimated the peak spectral sensitivity of observed opsin alleles in each population
238 (*following* (Jacobs et al., 2017)) and determined the difference between the two alleles with
239 maximum and minimum peak spectral sensitivities. These values, along with a total number of
240 observed alleles, were used in downstream analyses as proxies for enhanced trichromatic color
241 vision. Trichromatic color vision is most optimal with more widely separated photopigments
242 (e.g., (Osorio et al., 2004)). All else being equal, a greater number of opsin alleles results in an

243 increased proportion of heterozygous (trichromatic) females in a population.

244

245 *Analyses*

246 Climate and body size effects on pelage brightness and hue

247 We conducted four principal component analyses (PCAs): two across Indriidae and two
248 within *Propithecus*. One was for all the brightness variables across body regions and a second for
249 all the hue variables across body regions for Indriidae, to test specific hypotheses related to each
250 and to reduce the dimensionality of the data. We then ran two additional albeit similar PCAs
251 within only the *Propithecus* genus—given that the *Propithecus* genus is more widely
252 geographically distributed than either *Avahi* or *Indri*. We removed any variables with strongly
253 correlated vectors in the PCAs and then re-ran them to obtain the final PC values. We only used
254 the resulting PC values with eigenvalues over one as our dependent variables.

255 To test the effects of climate on pelage color while accounting for the evolutionary
256 relatedness of taxa, we used phylogenetic generalized linear mixed models (PGLMM) using
257 Markov chain Monte Carlo algorithms (MCMC) via the 'MCMCglmm' package in R (Hadfield,
258 2010). Our Indriidae phylogeny was based on a previously published lemur phylogeny that
259 contains a complete picture of Indriidae evolution (Herrera & Dávalos, 2016). We assigned the
260 phylogeny to the 'pedigree' argument in MCMCglmm, and the resulting matrix was used to
261 weigh the error structure of the model. Similar methodologies have been used to test the effects
262 of climate variables on bumblebee body size (Ramírez-Delgado et al., 2016) and frog vocal
263 signals (McLean et al., 2013). Each model included one color PC value as the dependent variable
264 and the bioclimatic variables (SI 5) and body size as independent variables, with species and
265 phylogeny considered random factors. We log-transformed PC values, bioclimatic variables, and

body size to achieve normality. All models ran for 5,000,000 iterations after a burn-in of 500,000 iterations and a thinning interval of 500 using flat priors. We assured effective sampling sizes were adequate for all our models (i.e., ESS virtually equal to MCMC sample size) (Villemereuil & Nakagawa, 2014).

We assigned statistical significance when pMCMC ≤ 0.05 (which is equivalent to a p-value (Villemereuil & Nakagawa, 2014)) and when the confidence interval for a given variable did not include zero (Ramírez-Delgado et al., 2016). To estimate what fraction of the pelage variation was attributable to phylogenetic relatedness, we calculated H^2 from Lynch (Lynch, 1991) (equivalent to Pagels's λ) which corresponds to the degree of variation in a given trait attributable to phylogenetic relatedness (Hansen & Orzack, 2005; Kamilar & Cooper, 2013). We ran the models across the whole Indriidae family and within the *Propithecus* genus. Using G*Power analysis (Faul et al., 2009), we estimated the PGLMMs would detect a small effect ((Indriidae, 0.25)-(*Propithecus*, 0.35)) with ≈80% power.

Climate and body size effects on pelage density

We conducted two principal component analyses (PCA) of hair and follicle density values: one across all Indriidae taxa and a second within the *Propithecus* genus. We removed any variables whose vectors strongly correlated in each of the PCAs. We used the resulting PC values with eigenvalues over one as dependent variables in our PGLMM models, following the methodology outlined above (see: climate and body size effects on pelage brightness and hue). Using G*Power analysis (Faul et al., 2009), we estimated the Indriidae PGLMM would detect a small effect (0.35), and the *Propithecus* PGLMM would detect a moderate effect (0.50) with ≈80% power. We also conducted an Analysis of Variance (ANOVA) to test for differences

between hair or follicle density across distinct body parts.

Polymorphic trichromacy and pelage hue variation

We ran one PCA on hue variables among a subset of individuals from which we had paired opsin genotypes and pelage measurements from the same population. We used any PCs with eigenvalues over one as the dependent variable in our linear models. To estimate the relationship between pelage hue and color vision, we conducted both (1) a simple linear regression and (2) PGLMM. Due to the small sample size (n = 10 localities/populations) (SI 6), we assumed that the "true" result likely fell between a model where lambda = 0 (simple linear model) and one where lambda = 1 (PGLMM). We followed the methods described previously, except we used 'spectral sensitivity range' (i.e., difference in opsin spectral sensitivity) and the 'total number of opsin alleles' as our independent variables. Despite the low sample size, using G*Power analysis (Faul et al., 2009), we estimated the simple linear model would detect a moderate effect (0.65) with ≈80% power.

Results

Climate and body size effects on pelage brightness and hue

Across Indriidae

Across Indriidae, the first PC for the brightness PCA explained ≈61% of the variation (SI 7). The highest loadings on PC1 were hindlimb, tail, and cheek brightness (SI 8). We found a statistically significant and positive association between hair brightness and precipitation seasonality (Table 1). Thus, darker pelage across Indriidae is associated with forests of lower

312 precipitation seasonality (i.e., higher rainfall, more humid) (Figure 2A). Brightness across
313 Indriidae exhibited a moderate phylogenetic signal (0.68) (Table 1). On the hue PCA, the first
314 three PCs explained ≈68% of the variation (SI 9, SI 10). The highest loadings were forelimb,
315 hindlimb and ventral torso hue (PC1), cheek and ventral torso (PC2), as well as crown hue (PC3)
316 (SI 10). We found a statistically significant relationship between PC1 and PC2 with precipitation
317 seasonality (Table 2). Indriidae with redder pelage hues live in regions that experience less
318 seasonality (i.e., higher rainfall) (Figure 3, SI 24). Hue values across Indriidae exhibited low to
319 moderate phylogenetic signal (0.25-0.48) (Table 2).
320
321 Within *Propithecus*
322 For the brightness PCA, the first PC explained ≈70% of the variation within *Propithecus*
323 (SI 11). The highest loadings on PC1 were hindlimb, dorsal torso, and forelimb brightness (SI
324 12). We found a statistically significant and positive association between hair brightness and
325 mean annual temperature (Table 1). Thus, darker pelage within *Propithecus* is associated with
326 colder forests (Figure 2B). Brightness across *Propithecus* exhibited a high phylogenetic signal
327 (0.90) (Table 1). For the hue PCA, the first three PCs explained ≈80% of the variation within
328 *Propithecus* (SI 13, SI 14). The highest loadings were forelimb, dorsal torso, and hindlimb hue
329 (PC1), cheek, ventral torso, and hindlimb hue (PC2), and crown hue (PC3) (SI 14). We found a
330 statistically significant relationship between PC2 and mean annual temperature, precipitation
331 seasonality, precipitation of the wettest month, and body size (Table 3). Thus, redder hues within
332 *Propithecus* are associated with lower precipitation seasonality (and higher rainfall). We found
333 no statistically significant relationships between either PC1 or PC3 with the tested variables.
334 There was low to moderate phylogenetic signal for hair hue within *Propithecus* (0.22-0.63)

335 (Table 3).

336

337 *Climate and body size effects on pelage density*

338 Across Indriidae

339 Across Indriidae, the first three PCs explained ≈70% of the variation (SI 15, SI 16). The
340 highest loadings were forelimb, hindlimb, and crown follicle density (PC1), ventral torso hair
341 density and crown and hindlimb follicle density (PC2), and dorsal torso hair density (PC3) (SI
342 16). We found a statistically significant relationship between PC1 and precipitation seasonality
343 as well as between PC3 and body size (Table 4). Specifically, the results suggest that in forests
344 with high precipitation seasonality (dryer, open forests exposed to the sun) individuals exhibit an
345 increase of follicle density on the limbs and crown (Figure 4). Also, smaller taxa have the highest
346 hair density; and, larger individuals exhibit lower hair density on average (Figure 5). Pelage
347 density across Indriidae exhibited low phylogenetic signal (0.21-0.33) (Table 4). We also found a
348 statistically significant difference between hair density across body regions sampled (Table 5).
349 Specifically, we found the crown and forelimbs exhibit the greatest hair density, and the ventral
350 torso exhibits the least hair density (Figure 6A). However, we found no significant differences in
351 follicle density of regions sampled (Table 5, Figure 6B).

352

353 Within *Propithecus*

354 Within *Propithecus*, the first three PCs explained ≈70% of the variation (SI 17, SI 18).
355 The highest loadings were forelimb follicle density, crown hair density, and hindlimb follicle
356 density (PC1), crown and hindlimb follicle density as well as hindlimb hair density (PC2), and
357 ventral torso hair density (PC3) (SI 18). We found a statistically significant relationship between
358 PC1 and precipitation seasonality, similar to Indriidae (Table 6). However, unlike the Indriidae

results, none of the PCs were significant with body size. Though, we detected significant differences between hair density and distinct body regions (SI 19), and no differences were detected among follicle density within *Propithecus* (SI 19, SI 20).

Polymorphic trichromacy and pelage hue variation

For the hue PCA using only a subset of the data from *Indri* and *Propithecus*, the first two PCs explained ≈66% of the variation (SI 21). The highest loadings to PC1 were forelimb, dorsal torso, and hindlimb hue, and the highest loadings to PC2 were cheek, ventral torso, and hindlimb hue (SI 22). From the simple linear model (lambda = 0), we found a statistically significant relationship between PC1 with the difference in opsin spectral sensitivity ($p = 0.03$; $R^2 = .51$), but not with the overall number of alleles in the population (Table 7). Specifically, we found a significant negative linear relationship between spectral sensitivity and hue (Figure 7). Despite the smaller sample size of the PGLMM (lambda = 1), we detected a similar association that approaches statistical significance (pMCMC = 0.09) and only moderate phylogenetic signal (0.41) (SI 23).

Discussion

Our overarching goals were to examine 1) if Indriidae pelage traits varied across distinct phylogenetic scales and 2) if multiple non-exclusive selective pressures would impact the same trait. We found support for both; distinct aspects of pelage color and density in Indriidae and sifakas (genus *Propithecus*) vary with climate, body size, and/or color vision.

Climate and body size effects on pelage brightness and hue

Our first sub-aim sought to uncover how climate and body size influenced pelage

383 brightness and hue across two distinct scales (across a family [Indriidae] and within a genus
384 [*Propithecus*]). Our results show distinct trends across scales regarding dark pelage (i.e.,
385 brightness). Specifically, across Indriidae, greater brightness is associated with greater
386 precipitation seasonality (Table 1). Greater hue, similarly, is associated with less precipitation
387 seasonality across Indriidae and *Propithecus* (SI 24)) (Table 2). Thus, more pigmented coats
388 (i.e., individuals with blacker and redder hair) occur in regions of lower precipitation seasonality
389 (Figure 2A, Figure 3). Generally, in Madagascar, low precipitation seasonality is strongly and
390 negatively associated with high precipitation forests of the East (SI 24). The result for brightness
391 follows Gloger's rule, predicting an increase in eumelanin (i.e., black pigments) (Delhey, 2017).
392 Yet, within *Propithecus*, results indicate a relationship between brightness and mean annual
393 temperature (Table 1). Thus, dark-haired sifakas are generally associated with colder regions,
394 which serves as evidence of Bogert's rule (or the thermal melanism hypothesis) (Figure 2B)
395 (Bogert, 1949).

396 Recent work highlights that discovering evidence for Bogert's or Gloger's rule may
397 merely reflect differences in geographic space, scale, and climate gradients (Delhey et al., 2019).
398 We show in this analysis that different effects can be detected across the primate coat, depending
399 on the sampling scale. Additionally, the strength of selective pressures acting on pelage may also
400 play a role in detecting either rule. For example, if the need to camouflage or avoid parasites is
401 high, rainfall (which predicts Gloger's rule) may strongly affect pelage color (da Silva et al.,
402 2016). This is because higher rainfall may also be associated with higher loads of parasites
403 (Shearer & Ezenwa, 2020) or may indicate low light forested environments that enhance crypsis
404 for dark animals (Caro, 2005; Delhey, 2018). In contrast, if the need for thermoregulation is
405 high, temperature (which predicts Bogert's rule) may have a more substantial effect on pelage

color than rainfall (Galván et al., 2018). It is hypothesized that black colors aid with thermoregulation in colder climates since they likely increase absorption of ultraviolet rays. While this has been documented widely in ectoderms and recently in birds (Bishop et al., 2016; Bogert, 1949; Clusella Trullas et al., 2007; Delhey et al., 2019; Xing et al., 2016), to date, our results serve as the first empirical evidence for Bogert's rule in mammals. Notably, the range of temperatures occupied by *Propithecus* species (≈10-27ºC) corresponds exceptionally well to the range at which Bogert's rule is expected to influence plumage color (≈10-25ºC) in passerines (Delhey et al., 2019). At this temperature range there is much nuance in the climatic space between temperature and precipitation, which is in turn is hypothesized to influence the rate of diversification and maintenance of species barriers (Delhey et al., 2019; Martin et al., 2010). Insights from other primate species may further elucidate the importance of Bogert's and Gloger's rules to broader primate evolution.

Both body size and phylogeny seem to have minimal impact on pelage color. First, body size only influenced hair hue across the *Propithecus* clade and otherwise did not affect our coloration models across either scale (Table 2, Table 3). At first glance, smaller individuals seem to exhibit redder hues; however, this trend is driven mostly by *Propithecus* species on the western side of the island. This may indicate subtler variation between species that our analysis does not capture. However, these results may also reflect broader climatic trends, variations in color vision (addressed below), or is perhaps the product of our body size sampling methodology. Second, most of the coloration traits we sampled exhibited low to moderate phylogenetic signals. Our brightness models, on the other hand, had a high phylogenetic signal (≈0.80). Thus, brightness may implicate genetic drift (Losos, 2008; Revell et al., 2008). However, it is well established that primate coat color exhibits little to no phylogenetic signal

429 and is a poor marker of phylogeny (Bell et al., 2021). An alternative explanation for such a high
430 signal is that it is an "artificial" result from taxonomic inflation that merely reflects patterns of
431 geographic variation (Kamilar & Muldoon, 2010).
432
433 *Climate and body size effects on pelage density*
434 Our second sub-aim sought to uncover how climate and body size influenced pelage hair
435 and follicle density across two distinct scales (across a family [Indriidae] and within a genus
436 [*Propithecus*]). We predicted that body size would affect density because these variables are
437 associated across primates. Body size may also have been one of the factors influencing the
438 reduction of the hairy coat in hominins (Sandel, 2013; Schwartz & Rosenblum, 1981). We found
439 support for this prediction across Indriidae (Table 4). Specifically, higher hair density is
440 associated with smaller body sizes (*Avahi*), and lower hair density is found in larger animals
441 across Indriidae (Figure 4). One explanation for this result may be that interfollicular distance
442 increases as surface area increases, thus, decreasing hair density in larger animals (Sandel, 2013).
443 In addition, this relationship may provide thermoregulatory benefits since larger animals may
444 struggle more to dissipate heat (Schwartz & Rosenblum, 1981). Our models show that climate
445 also influences pelage variation across Indriidae. Limb and crown follicle density increases as
446 precipitation seasonality increases (i.e., shifting to dry open habitats) (Table 4; Figure 4).
447 Interestingly, the crown and forelimbs are also the regions that exhibit the highest degree of hair
448 density (Figure 6A)—but not follicle density (Figure 6B). Thus, there are likely two mechanisms
449 to increase density: (1) increase hair follicle density or (2) increase the number of hairs emerging
450 from each follicle. Since follicle density is determined in early embryogenesis, follicle density
451 may be more strongly genetically determined than hair density (which may be more plastic to

452 rapid environmental changes, such as seasonality) (Tapanes et al., 2021). Alternatively, follicle
453 density may be easier to measure without error and could be a more reliable estimate for
454 'hairiness.'

455 Nevertheless, the shift towards drier habitats exposed to more sun (such as Western spiny
456 thickets) leads to an increase in follicle density in the limbs and crown (Figure 4), where hair
457 density is already the highest of all regions (Figure 6A). Since all Indriidae are vertical clingers
458 and leapers, the crown and upper limbs are the most directly impacted by the sun's rays—as they
459 are known to hold up their arms while jumping bipedally. Thus, increased hair density in these
460 regions may aid individuals in this clade with protection from ultraviolet rays (and/or protect the
461 underlying skin from abrasion in spiny thickets). We consider this density pattern may help
462 prevent photolysis of folate, an essential metabolite in the formation of the embryonic neural
463 tube. Protection against folate leaching was likely a selection target in the evolution of high
464 melanization within the skin of humans living in high UV areas (Jablonski & Chaplin, 2000). In
465 humans, lower levels of folate (or folate deficiency) are also often significantly associated with
466 hair loss (Almohanna et al., 2019; Ertug, 2018), and folate may play a significant role within the
467 hair follicle (Durusoy et al., 2009). Since the skin of most Indriidae is already highly melanized,
468 it is not surprising that populations exposed to hotter environments and more direct sun often
469 have lighter coats (Figure 2B, Figure 3)—potentially to prevent overheating due to lack of sweat
470 glands. We note that although *Avahi* is nocturnal relative to *Propithecus* and *Indri*, recent work
471 explains their activity patterns may be more accurately described as "cathermality sensu *lato.*"
472 Mainly this is because certain species are active across daylight hours, depending on the lunar
473 phase (Campera et al., 2019). Therefore, implications of the potential function of the pelage
474 pattern detected across the family is not solely relegated to *Propithecus* and *Indri*. However, we

note that other aspects of hair morphology that we did not measure (length, curvature) may influence the strength of this selective pressure differently in distinct genera (Lasisi, 2021). Future studies should consider smaller phylogenetic scales, and other aspects of hair morphology (e.g., length) and climate (e.g., wind speed). Nonetheless, the pattern that emerges from this data may signal that variation in hair density (i.e., higher hair density in the scalp) across the human body may have occurred early on as an early mechanism to prevent folate leaching from key body regions exposed to direct UV rays. This body hair pattern potentially preceded the evolution of "naked" skin and sweat glands.

Our data is also rare evidence supporting the body cooling hypothesis—from the perspective of hair density in non-human primates. The body cooling hypothesis (Wheeler, 1985; 1992) argued that bipedal hominins evolved naked skin to allow for evaporative cooling. However, Wheeler (1985, 1992) also argued as part of this hypothesis that bipedal hominins likely retained hair on the crown and shoulders to protect those areas from UV exposure. Indriidae, presenting similar postural locomotion to humans, exhibit follicle density increases in their body regions most exposed to potential UV damage. Indriidae present a unique opportunity to comparatively study potential tradeoffs between folate levels, hair density, hair color, and thermoregulation across and within populations to clarify potential mechanisms driving this pattern of hair variation in upright primates.

Our results indicate that body size is also likely contributing to hair density variation (Figure 5). However, the smallest primates within the Indriidae clade are also nocturnal; larger-bodied Indriidae are diurnal. Thus, "body size" is likely confounded by activity cycle. Our results show that within *Propithecus* alone, there was no variation in hair density detected with body size—but there was with climate (Table 6). This may be due to a smaller sample size

498 available for *Propithecus* density which we estimated would not pick up small effects (G* power
499 analyses detailed in methods). Alternatively, at smaller phylogenetic scales, other aspects of hair
500 morphology that we did not measure (e.g., overall shape, length, thickness) may directly relate to
501 body size best at a smaller phylogenetic scale. For example, there are no differences in hair
502 density between chimpanzees and humans, but there are significant differences in gland density,
503 sweat production, and overall hair morphology (Kamberov et al., 2018). Hair and follicle density
504 was likely one of a few aspects of hair evolution that were potentially malleable and allowed
505 rapid adaptation to changing climatic environments for hominins. More research is needed across
506 non-human and human primate hair to understand why and how humans retained hair in the
507 places they did (e.g., scalp, pubic)—a critical part of the story in the evolution of our apparent
508 "nakedness."
509
510 *Polymorphic trichromacy and pelage hue variation*
511 Our third sub-aim sought to understand the relationship between color vision and pelage
512 hue in diurnal genera. We found support for our prediction that populations with enhanced
513 capacity for trichromatic color vision would also contain individuals with redder pelage (*as*
514 *hypothesized in* (Sumner & Mollon, 2003)). Many primates are unique among placental
515 mammals in having trichromatic color vision, a feature that is thought to be advantageous for
516 foraging on "red" foods (i.e., ripe fruit, young leaves), detecting predators, and/or tracking
517 conspecifics (Kawamura et al., 2012; Surridge et al., 2003). Indeed, reddish skin coloration
518 observed in many primate species is thought to play a salient role in conspecific signaling for
519 primates (Moreira et al., 2019). However, previous support for the coevolution of red hair and
520 trichromacy in primates is mixed (Fernandez & Morris, 2007; Kamilar et al., 2013). Our results

521 indicate a significant positive relationship between hue ('redness') and measures of enhanced
522 trichromacy in Indriidae (Table 7). The similarity in results between both models (lambda=0 vs.
523 lambda=1) indicates a likely significant relationship between hue and opsin genotype variation in
524 diurnal Indriidae. Specifically, red hues are more likely to occur when there is a larger difference
525 in spectral sensitivity between opsin alleles (Figure 7), suggesting increased discriminability of
526 such hues. Results across Indriidae, which exhibits more subtle inter- and intra-species variation
527 in trichromacy than has been previously considered, suggests that there may be a more complex
528 and nuanced coevolutionary relationship between red hair coloration in primates and
529 trichromatic color vision that deserves further attention (Table 7).
530
531 *Conclusions*
532 Climate, body size, and color vision all impact hair variation across Indriidae, but the
533 extent that each exerts its influence on the phenotype varies by sampled phylogenetic scale.
534 These results have considerable implications for our understanding of primate (including human)
535 hair evolution because it suggests that larger macro-scale trends detected across primates may
536 not sufficiently explain variation within a genus, species, or population. Understanding wild non-
537 human primate hair can also potentially help shed light on the evolution of hominin hair. Further
538 work on primate hair should sample across smaller geographic or phylogenetic scales and from
539 diverse non-human and human populations.
540
541 **Acknowledgments**
542 We thank the American Museum of Natural History, the Smithsonian National Museum of
543 Natural History, and Harvard University's Museum of Comparative Zoology. Special thanks to

museum staff that helped with *Propithecus* collections, including Ian Tattersall, Darrin Lunde, Mark Omura, Eleanor Hoeger, and Marisa Surovy. We also thank the Government of Madagascar (Ministry of the Environment and Sustainable Development), SADABE, Madagascar Biodiversity Partnership (MBP), Omaha Zoo, the University of Antananarivo, and Anthropobiologie et Développement for facilitation and partnership. We thank members of GW PGL and Utah PEGL labs for relevant discussions and feedback on ideas presented here. Illustrations copyright 2020 Stephen D. Nash/IUCN SSC Primate Specialist Group, used and modified with permission. The findings and conclusions in this article are those of the author(s) and do not necessarily represent the views of the U.S. Fish and Wildlife Service. The work was supported by the Leakey Foundation, the Wenner Gren Foundation, the National Science Foundation (BCS #1546730, BCS #1606360), the George Washington University, Northern Illinois University, National Geographic CRE, Eppley Fund for Research, Primate Conservation Inc., and IdeaWild. Field work to collect biological samples was supported by Conservation International, Margot Marsh Biodiversity Foundation, and The Ahmanson Foundation. The funders had no role in study design, data collection and analysis, decision to publish, or preparation of the manuscript.

References

Allen, W. L., & Higham, J. P. (2013). Analyzing visual signals as visual scenes. *American Journal of Primatology*, *75*(7), 664–682.

Almohanna, H. M., Ahmed, A. A., Tsatalis, J. P., & Tosti, A. (2019). The role of vitamins and minerals in hair loss: A review. *Dermatology and Therapy*, *9*(1), 51–70.

Avram, M. R., & Rogers, N. E. (2009). The use of low-level light for hair growth: Part i. *Journal of Cosmetic and Laser Therapy*, *11*(2), 110–117.

Barrett, R. D. H., Laurent, S., Mallarino, R., Pfeifer, S. P., Xu, C. C. Y., Foll, M., … Hoekstra, H. E. (2019). Linking a mutation to survival in wild mice. *Science*, *363*(6426), 499–504.

Bell, R. B., Bradley, B. J., & Kamilar, J. M. (2021). The evolutionary ecology of primate hair coloration: A phylogenetic approach. *Journal of Mammalian Evolution, 28,* 911-927.

Bergman, T. J., & Beehner, J. C. (2008). A simple method for measuring colour in wild animals: validation and use on chest patch colour in geladas (*Theropithecus gelada*). *Biological Journal of the Linnean Society*, *94*(2), 231–240.

Best, A., Lieberman, D., & Kamilar, J. (2019). Diversity and evolution of human eccrine sweat gland density. *Journal of Thermal Biology*, *84*, 331–338.

Bishop, T. R., Robertson, M. P., Gibb, H., van Rensburg, B. J., Braschler, B., Chown, S. L., … Parr, C. L. (2016). Ant assemblages have darker and larger members in cold environments. *Global Ecology and Biogeography*, *25*(12), 1489–1499.

Bogert, C. M. (1949). Thermoregulation in reptiles, a factor in evolution. *Evolution*, *3*, 195–211.

Bradley, B. J., Walsh, S., Nishimura, A., Karlsson, J., & Kamilar, J. M. (2014). The evolution of primate pelage: Morphological analysis of museum research skins. *Program of the 83rd Annual Meeting of the American Association of Physical Anthropologists*, *153*(S58).

Campera, M., Balestri, M., Chimienti, M., Nijman, V., Nekaris, K.A.I., & Donati, G. (2019). Temporal niche seperation between the two ecologically similar nocturnal primates *Avahi meridionalis* and *Lepilemur fleuretae*. *Behavioral Ecology and Sociobiology*, *73*, 55.

Caro, T. (2005). The adaptive significance of coloration in mammals. *BioScience*, *55*(2), 125-136.

Chaplin, George, Jablonski, Nina G., & Cable, T. N. (1994). Physiology, thermoregulation and bipedalism. *Journal of Human Evolution*, *27*(6), 497–510.

Clusella Trullas, S., van Wyk, J. H., & Spotila, J. R. (2007). Thermal melanism in ectotherms. *Journal of Thermal Biology*, *32*(5), 235–245.

Cuthill, I. C., Allen, W. L., Arbuckle, K., Caspers, B., Chaplin, G., Hauber, M. E., … Caro, T. (2017). The biology of color. *Science*, *357*(6350), aan0221.

da Silva, L. G., de Oliveira, T. G., Kasper, C. B., Cherem, J. J., Moraes, E. A., Paviolo, A., & Eizirik, E. (2016). Biogeography of polymorphic phenotypes: Mapping and ecological modelling of coat colour variants in an elusive Neotropical cat, the jaguarundi (*Puma yagouaroundi*). *Journal of Zoology*, *299*(4), 295–303.

Delhey, K. (2017). Gloger's rule. *Current Biology*, *27*(14), R689–R691.

Delhey, K. (2018). Darker where cold and wet: Australian birds follow their own version of Gloger's rule. *Ecography*, *41*(4), 673–683.

Delhey, K., Dale, J., Valcu, M., & Kempenaers, B. (2019). Reconciling ecogeographical rules: rainfall and temperature predict global colour variation in the largest bird radiation. *Ecology Letters*, *22*(4), 726–736.

Durusoy, C., Ozenli, Y., Adiguzel, A., Budakoglu, I. Y., Tugal, O., Arikan, S., & Uslu, A. (2009). The role of psychological factors and serum zinc, folate and vitamin B 12 levels in

the aetiology of trichodyni: A case–control study. *Clinical and Experimental Dermatology, 34*(7), 789–792.

Dutton, A., Christopher, J., & Randall, E. (2003). Biomedical evaluation of free-ranging ring-tailed lemurs (*Lemur catta*) in Tsimanampetsotsa Strict Nature Reserve, Madagascar. *Journal of Zoo and Wildlife Medicine*, *34*(1), 16–24.

Ertug, E. Y. (2018). Reduced ferritin, folate, and vitamin B12 levels in female patients diagnosed with telogen effluvium. *International Journal of Medical Biochemistry, 1*(3), 0–2.

Faul, F., Erdfelder, E., Buchner, A., & Lang, A. G. (2009). Statistical power analyses using G*Power 3.1: Tests for correlation and regression analyses. *Behavior Research Methods*, *41*(4), 1149–1160.

Fernandez, A. A., & Morris, M. R. (2007). Sexual selection and trichromatic color vision in primates: Statistical support for the preexisting-bias hypothesis. *American Naturalist*, *170*(1), 10–20.

Fratto, M. A., & Davis, A. K. (2011). Do black-furred animals compensate for high solar absorption with smaller hairs? A test with a polymorphic squirrel species. *Current Zoology*, *57*(6), 731–736.

Galván, I., Rodríguez-Martínez, S., & Carrascal, L. M. (2018). Dark pigmentation limits thermal niche position in birds. *Functional Ecology*, *32*(6), 1531–1540.

Glogger, C.W.L. (1833). Das Abändern der Vögel durch Einfluss des Kilmas. Breslau: August Schulz. & Co.

Godfrey, L.R., Samonds, K.E., Jungers, W.L., & Sutherland, M.R. (2001). Teeth, brains, and primate life histories. *American Journal of Physical Anthropology*, *114*(3), 192-214.

Guevara, E.E. (2018). Genomics of primate longevity (Publication No. 13141656). [Doctoral

dissertation, Yale University]. ProQuest Dissertations and Theses.

Hadfield, J. D. (2010). MCMC methods for multi-response generalized linear mixed models: The MCMCglmm R package. *Journal of Statistical Software*, *33*(2), 1–22.

Hansen, T. F., & Orzack, S. H. (2005). Assessing current adaptation and phylogenetic inertia as explanations of trait evolution: The need for controlled comparisons. *Evolution*, *59*(10), 2063-2072.

Herrera, J. P., & Dávalos, L. M. (2016). Phylogeny and divergence times of lemurs inferred with recent and ancient fossils in the tree. *Systematic Biology*, *65*(5), 772–791.

Hijmans, R. J., & Etten, J. V. (2012). Raster: Geographic analysis and modeling with raster data. *R package version 2.0-12.*

Hoekstra, H. E., Krenz, J. G., & Nachman, M. W. (2005). Local adaptation in the rock pocket mouse (*Chaetodipus intermedius*): Natural selection and phylogenetic history of populations. *Heredity*, *94*(2), 217–228.

Irwin, M. T., Junge, R. E., Raharison, J. L., & Samonds, K. E. (2010). Variation in physiological health of diademed sifakas across intact and fragmented forest at Tsinjoarivo, eastern Madagascar. *American Journal of Primatology*, *72*(11), 1013–1025.

Jablonski, N. G., & Chaplin, G. (2000). The evolution of human skin coloration. *Journal of Human Evolution*, *39*(1), 57–106.

Jacobs, R. L., MacFie, T. S., Spriggs, A. N., Baden, A. L., Morelli, T. L., Irwin, M. T., … Bradley, B. J. (2017). Novel opsin gene variation in largebodied, diurnal lemurs. *Biology Letters*, *13*(3), 1–6.

Jacobs, R. L., Spriggs, A. N., MacFie, T. S., Baden, A. L., Irwin, M. T., Wright, P. C., … Bradley, B. J. (2016). Primate genotyping via high resolution melt analysis: rapid and

reliable identification of color vision status in wild lemurs. *Primates*, *57*(4), 541–547.

Jacobs, R. L., Veilleux, C. C., Louis, E. E., Herrera, J. P., Hiramatsu, C., Frankel, D. C., … Bradley, B. J. (2019). Less is more: lemurs (*Eulemur* spp.) may benefit from loss of trichromatic vision. *Behavioral Ecology and Sociobiology*, *73*, 22.

Kamberov, Y. G., Guhan, S. M., DeMarchis, A., Jiang, J., Wright, S. S., Morgan, B. A., … Lieberman, D. E. (2018). Comparative evidence for the independent evolution of hair and sweat gland traits in primates. *Journal of Human Evolution*, *125*, 99–105.

Kamilar, J. M., & Bradley, B. J. (2011). Interspecific variation in primate coat colour supports Gloger's rule. *Journal of Biogeography*, *38*(12), 2270–2277.

Kamilar, J. M., & Cooper, N. (2013). Phylogenetic signal in primate behaviour, ecology and life history. *Philosophical Transactions of the Royal Society of London. Series B, Biological Sciences*, *368*, 20120341.

Kamilar, J. M., Heesy, C. P., & Bradley, B. J. (2013). Did trichromatic color vision and red hair color coevolve in primates? *American Journal of Primatology, 75*(7), 740-751.

Kamilar, J. M., & Muldoon, K. M. (2010). The climatic niche diversity of Malagasy primates: A phylogenetic perspective. *PLoS ONE*, *5*(6), e11073.

Kawamura, S., Hiramatsu, C., Melin, A. D., Schaffner, C. M., Aureli, F., & Fedigan, L. M. (2012). Polymorphic color vision in primates: Evolutionary considerations. In H. Hirai, H. Imai, & Y. Go (Eds.), *Post-Genome Biology of Primates* (pp. 93-120). Tokyo: Springer.

Kendal, D., Hauser, C. E., Garrard, G. E., Jellinek, S., Giljohann, K. M., & Moore, J. L. (2013). Quantifying plant colour and colour difference as perceived by humans using digital images. *PLoS ONE*, *8*(8), e72296.

King, T., Rakotonirina, L. H. F., Rakotoarisoa, A. H., Razafindramanana, J., & Ratsimbazafy, J.

(2014). Distributional limits and melanism in the south-west of the range of the crowned sifaka (*Propithecus coronatus*), Madagascar. *Primate Conservation*, *28*(1), 55–64.

Lasisi, T., Ito, S., Wakamatsu, K., & Shaw, C. N. (2016). Quantifying variation in human scalp hair fiber shape and pigmentation. *American Journal of Physical Anthropology*, *160*(2), 341–352.

Lasisi, T. (2021). The genetic architecture and evolutionary function of human scalp hair morphology (Publication No. 28841761). [Doctoral dissertation, Penn State University]. ProQuest Dissertations and Theses.

Lawler, R.R., Caswell, H., Richard, A.F., Ratsirarson, J., Dewar, R.E., & Schwartz, M. 2009. Demography of Verreauix's sifaka in a stochastic rainfall environment. *Oecologia*, 161, 491-504.

Lehman, S. M. (2007). Ecological and phylogenetic correlates to body size in the Indriidae. *International Journal of Primatology*, *28*(1), 183–210.

Lewis, R. J., & Van Schaik, C. P. (2007). Bimorphism in male verreaux's sifaka in the Kirindy Forest of Madagascar. *International Journal of Primatology*, *28*(1), 159–182.

Losos, J. B. (2008). Phylogenetic niche conservatism, phylogenetic signal and the relationship between phylogenetic relatedness and ecological similarity among species. *Ecology Letters*, *11*(10), 995–1003.

Lynch, M. (1991). Methods for the analysis of comparative data in evolutionary biology. *Evolution*, *45*(5), 1065–1080.

Martin, P.R., Montgomerie, R., Lougheed, S.C. (2010). Rapid sympatry explains greater color pattern divergence in high latitude birds. *Evolution, 64*(2), 336-347.

McLean, M. J., Bishop, P. J., & Nakagawa, S. (2013). Assessing the patterns of evolution in

anuran vocal sexual signals. *Evolutionary Biology*, *40*(1), 141–149.

Mittermeier, Russell A., Louis, Jr., Edward E., Richardson, M., Schwitzer, C., Langrand, O., Rylands, Anthony B., … MacKinnon, K. C. (Eds.) (2010). *Lemurs of Madagascar* (3rd ed.). New York: Conservation International.

Moreira, L. A. A., Duytschaever, G., Higham, J. P., & Melin, A. D. (2019). Platyrrhine color signals: New horizons to pursue. *Evolutionary Anthropology*, *28*(5), 236–248.

Norton, H. L., Edwards, M., Krithika, S., Johnson, M., Werren, E. A., & Parra, E. J. (2016). Quantitative assessment of skin, hair, and iris variation in a diverse sample of individuals and associated genetic variation. *American Journal of Physical Anthropology*, *160*(4), 570–581.

Osorio, D., Smith, A. C., Vorobyev, M., & Buchanan-Smith, H. M. (2004). Detection of fruit and the selection of primate visual pigments for color vision. *American Naturalist*, *164*(6), 696–708.

Paus, R., & Foitzik, K. (2004). In search of the "hair cycle clock": A guided tour. *Differentiation*, *72*(9–10), 489–511.

Pebesma, E. J., & Bavand, R. S. (n.d.). Classes and methods for spatial data in R. *R News*, *5*(2), 9–13.

Petter, J. J., & Peyrieras, A. (1972). Melanization in the genus *Propithecus* Malagasey Lemur. *Journal of Human Evolution*, *1*(4), 379–388.

Post, P. W., Szabó, G., & Keeling, M. E. (1975). A quantitative and morphological study of the pigmentary system of the chimpanzee with the light and electron microscope. *American Journal of Physical Anthropology*, *43*(3), 435–443.

Rakotonirina, H., Kappeler, P. M., & Fichtel, C. (2017). Evolution of facial color pattern

complexity in lemurs. *Scientific Reports*, *7*(1), 1–11.

Rakotonirina, L. H. F., Randriantsara, F., Rakotoarisoa, A. H., Rakotondrabe, R., Razafindramanana, J., Ratsimbazafy, J., & King, T. (2014). A preliminary assessment of sifaka (*Propithecus*) distribution, chromatic variation and conservation in Western Central Madagascar. *Primate Conservation*, *28*(1), 43–53.

Ramírez-Delgado, V. H., Sanabria-Urbán, S., Serrano-Meneses, M. A., & Cueva del Castillo, R. (2016). The converse to Bergmann's rule in bumblebees, a phylogenetic approach. *Ecology and Evolution*, *6*(17), 6160–6169.

Revell, L. J., Harmon, L. J., & Collar, D. C. (2008). Phylogenetic signal, evolutionary process, and rate. *Systematic Biology*, *57*(4), 591–601.

Rowe, N. (1996). *The pictoral guide to the living primates*. East Hampton: Pagonias Press.

Sambrook, J., Fritch, E., & Maniatus, T. (1989). *Molecular cloning: a laboratory manual.* (2nd ed.). New York: Cold Spring Harbor Press.

Sandel, A. A. (2013). Brief communication: Hair density and body mass in mammals and the evolution of human hairlessness. *American Journal of Physical Anthropology*, *152*(1), 145–150.

Santana, S. E., Alfaro, J. L., Noonan, A., & Alfaro, M. E. (2013). Adaptive response to sociality and ecology drives the diversification of facial colour patterns in catarrhines. *Nature Communications*, *4*, 1–7.

Santana, S. E., Lynch Alfaro, J., & Alfaro, M. E. (2012). Adaptive evolution of facial colour patterns in Neotropical primates. *Proceedings. Biological Sciences / The Royal Society*, *279*(1736), 2204–2211.

Schmidt, M. (2011). Locomotion and postural behaviour. *Advances in Science and Research*,

5(1), 23–39.

Schwartz, G. G., & Rosenblum, L. A. (1981). Allometry of primate hair density and the evolution of human hairlessness. *American Journal of Physical Anthropology*, *55*(1), 9–12.

Seibert, H. C., & Steggerda, M. (1999). The size and shape of human head hair: Along its shaft. *The Journal of Heredity*, *33*(8), 302–304.

Shearer, C. L., & Ezenwa, V. O. (2020). Rainfall as a driver of seasonality in parasitism. *International Journal for Parasitology: Parasites and Wildlife*, *12*, 8–12.

Spriggs, A. N. (2017). Evolution of lemur pelage color variation (Publication No. 10682576). [Doctoral dissertation, University at Albany, State University of New York]. ProQuest Dissertations and Theses..

Steggerda, M., & Seibert, H. C. (1941). Size and shape of head hair from six racial groups. *Journal of Heredity*, *32*(9), 315–318.

Stevens, M., Párraga, C. A., Cuthill, I. C., Partridge, J. C., & Troscianko, T. S. (2007). Using digital photography to study animal coloration. *Biological Journal of the Linnean Society*, *90*(2), 211–237.

Stevens, M., Stoddard, M. C., & Higham, J. P. (2009). Studying primate color: towards visual system-dependent methods. *International Journal of Primatology*, *30*(6), 893–917.

Sumner, P., & Mollon, J. D. (2003). Colors of primate pelage and skin: Objective assessment of conspicuousness. *American Journal of Primatology*, *59*(2), 67–91.

Surridge, A. K., Osorio, D., & Mundy, N. I. (2003). Evolution and selection of trichromatic vision in primates. *Trends in Ecology and Evolution*, *18*(4), 198–205.

Tapanes, Elizabeth, Kamilar, Jason M, & Bradley, B. J. (2021). Molecular and cellular processes of pelage growth and pigmentation in primate evolution. In K.M. Pitirri, J.T. & Richtsmeier

(Eds.). *Evolutionary Cell Processes in Primates* (pp. 1–33). Boca Raton: CRC Press.

Tapanes, E., Irwin, M., Spriggs, Amanda Nicole, Kamilar, Jason M., & Bradley, B. J. (2018). Subtle sexual dichromatism and dimorphism detected in wild *Propithecus diadema*. *Program of the 87th Annual Meeting of the American Association of Physical Anthropologists*, *165*(S66).

Tattersall, I. (1986). Notes on the distribution and taxonomic status of some species of *Propithecus* in Madagascar. *Folia Primatologica*, *46*, 51–63.

Villemereuil, P. de, & Nakagawa, S. (2014). General quantitative genetic methods for comparative biology. In L.Z. Garamszegi (Ed.). *Modern Phylogenetic Comparative Methods and their Application in Evolutionary Biology* (pp. 287–304). Berlin: Springer.

Wheeler, P. E. (1985). The loss of functional body hair in man: the influence of thermal environment, body form and bipedality. *Journal of Human Evolution*, *14*(1), 23–28.

Wheeler, P. E. (1992). The influence of the loss of functional body hair on the water budgets of early hominids. *Journal of Human Evolution*, *23*(5), 379–388.

Winters, S., Allen, W., & Higham, J. (2020). The structure of species discrimination signals across a primate radiation. eLife, 9:e47428.

Xing, S., Bonebrake, T. C., Tang, C. C., Pickett, E. J., Cheng, W., Greenspan, S. E., … Scheffers, B. R. (2016). Cool habitats support darker and bigger butterflies in Australian tropical forests. *Ecology and Evolution*, *6*(22), 8062–8074.

Figure Legends

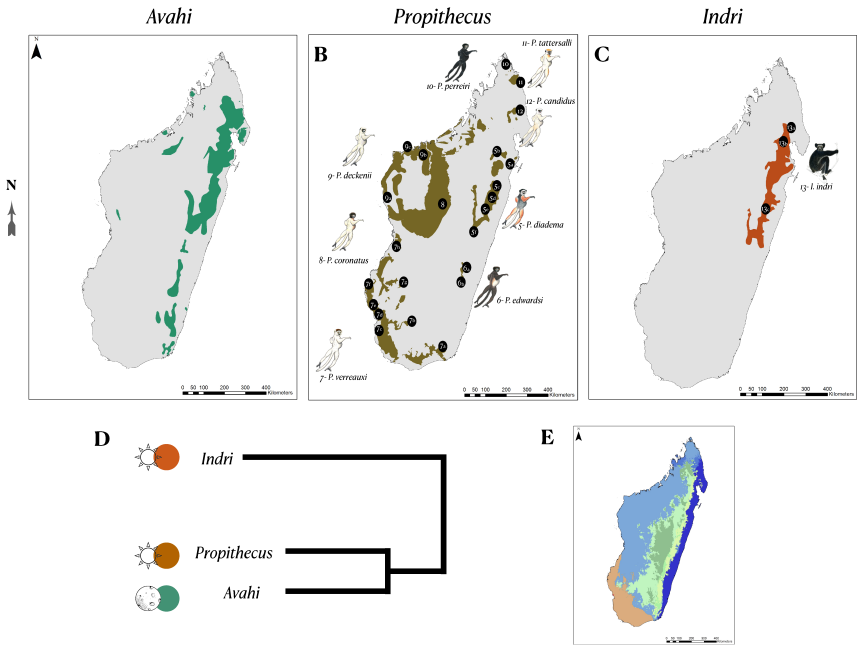

Figure 1 Indriidae species ranges and sampling localities for (A) *Avahi*, (B) *Propithecus*, and (C) *Indri*; along with a (D) cladogram, and (E) Koppen-climate zones that span the genera's distribution.

Key: *Avahi* spp. = (1a) Betampona, (1b) Sihanaka forest, (1c) Andasibe, (2) Forest west of Fort Dauphin, (3) Vondrozo, (4) Ankarafatsika; *Propithecus* spp. = (5a) Betampona, (5b) Zahamahena, (5c) Didy, (5d) Sihanaka forest, (5e) forest patch near Andasibe, (5f) Tsinjoarivo (eastern and western), (6a) Nandihizana, (6b) East of Farohny River, (7a) Mandrare Valley, (7b) Bevala East, (7c) Tsinanampetsotsa, (7d) Lower Ifaty, (7e) Ifaty, (7f) Lake Ihortry, (7g) Ankazoabo West, (7h) Upper Tsirbihina River, (8) Ambararatabe, (9a) Tsingy de Bemaraha, (9b) Tsingy de Namoraka, (9c) Baie de Baly Nat Park, (10) Reserve of Analamerana, (11) Forest fragment near Daraina, (12) Anjanaharibe-Sud Reserve; *Indri* indri = (13a) Anjanaharibe-Sud Reserve, (13b) 40 km West of Maroantsetra, (13c) Sihanaka forest

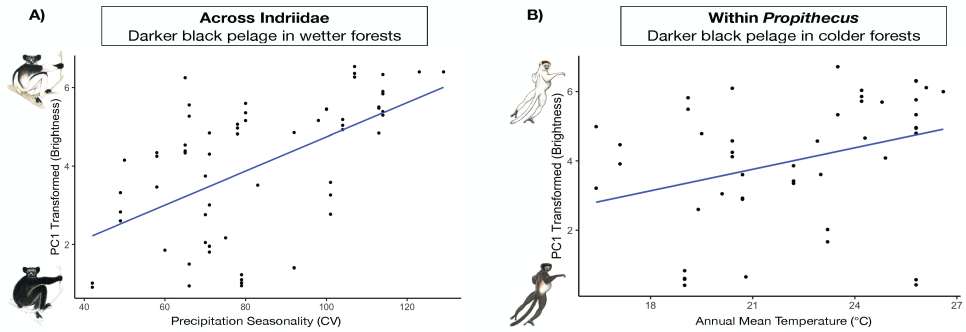

Figure 2 Plot of brightness across (A) the entire Indriidae family, in association with precipitation Seasonality (CV) (showing adherence to Gloger's Rule), and (B) only within the *Propithecus* genus, in association with Annual Mean Temperature (°C) (showing adherence to Bogert's Rule).

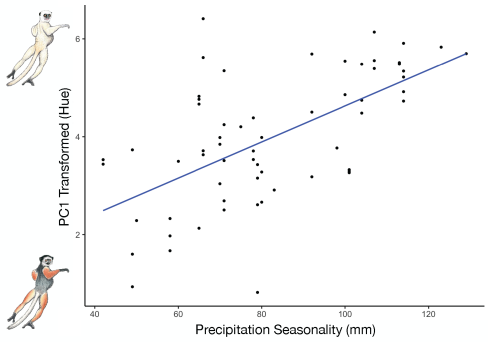

Figure 3 Plot of pelage hue trends across (A) the entire Indriidae family, in association with precipitation seasonality (mm) (showing adherence to Gloger's Rule). Results are similar within *Propithecus*.

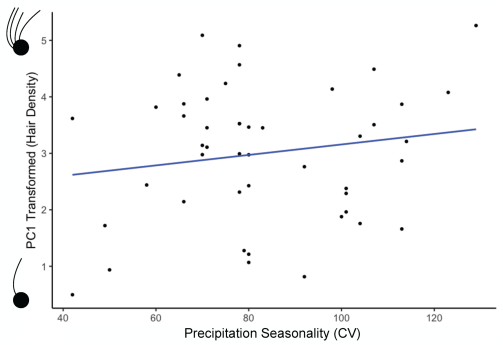

Figure 4 Plot of hair density trends. The relationship between PC1 and precipitation seasonality (CV) is significantly associated with hair density on the limbs and crown across the Indriidae family. Lower PC1 values are associated with lower hair density on the limbs and crown.

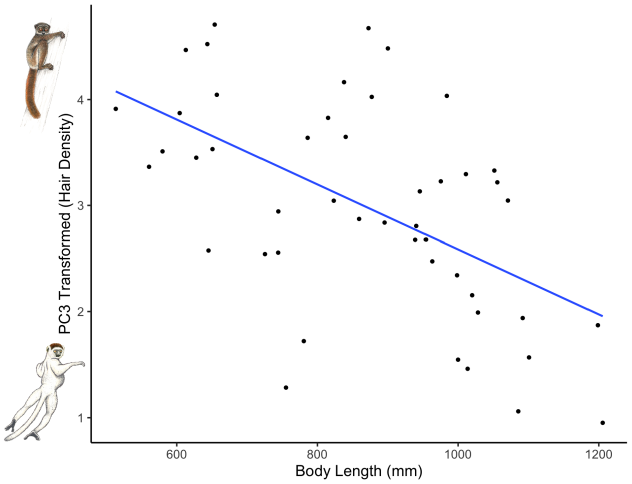

Figure 5 Plot of hair density trends. The relationship between PC3 and body length (capturing length, in mm) is significantly associated with hair density on the dorsal torso across Indriidae. Lower PC3 values are associated with lower hair density across the dorsal torso.

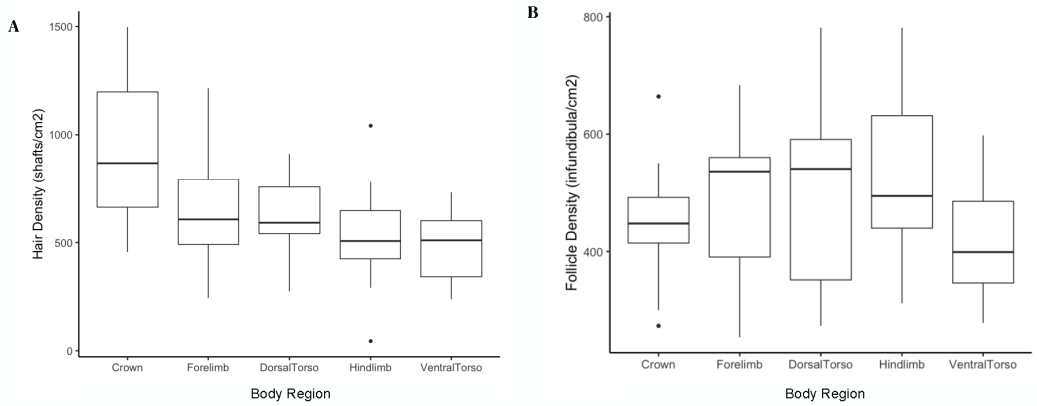

Figure 6 Boxplots illustrating variation in (A) hair density and (B) follicle density across body regions, for Indriidae. Black lines represent the average, and black dots represent outliers.

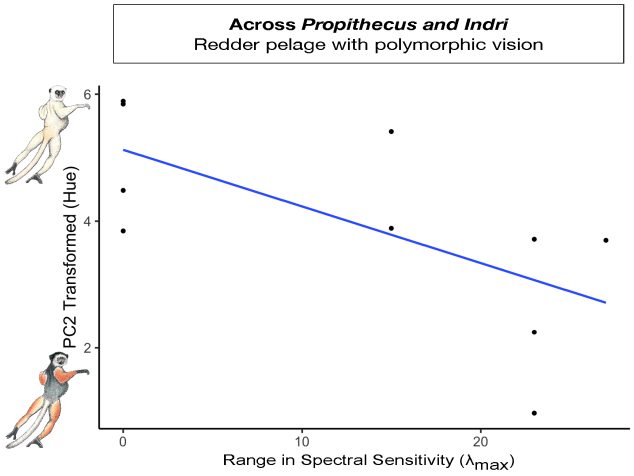

Figure 7 Plot of pelage hue trends across diurnal *Propithecus* and *Indri* genera, in association with the range (i.e., difference) in opsin peak spectral sensitivity.

843

844 **Table 1** Results of PGLMMs predicting hair brightness (RGB averages) across all Indriidae taxa

845 and only within *Propithecus*

Variable	Mean Est.	Lower CI	Upper CI	ESS	P MCMC
Across Indriidae (PC1; $H^2 = 0.666$)					
Intercept	-5.901	-15.911	4.432	9,000	0.242
BIO01	-0.540	-1.510	0.401	9,000	0.256
BIO04	0.901	-0.492	2.290	9,000	0.216
BIO07	-0.393	-2.264	1.396	9,000	0.662
BIO13	0.293	-0.171	0.762	9,000	0.218
BIO15	0.728	-0.016	1.431	9,000	**0.048**
Body size	0.010	-0.727	0.696	9,000	0.972
Within *Propithecus* (PC1; $H^2 = 0.902$)					
Intercept	0.710	-8.640	10.541	9,563	0.900
BIO01	-1.291	-2.064	-0.571	9,000	**0.002**
BIO04	-0.501	-1.920	0.863	9,410	0.471
BIO07	0.613	-0.921	2.176	9,000	0.430
BIO13	0.001	-0.398	0.436	9,000	0.999
BIO15	0.347	-0.289	0.988	9,000	0.284
Body size	0.527	-0.051	1.103	9,000	$0.075^{!}$

846 Bold values indicate $p < 0.05$, $^{!}$ indicates $p < 0.10$, H^2 is akin to phylogenetic signal

847

848

849

850

851

852

853

854

855

856

857

858

859 **Table 2** Results of PGLMMs predicting hair hue (RG ratio values) across all Indriidae taxa

Variable	Mean Est.	Lower CI	Upper CI	ESS	P MCMC
PC1; $H^2 = 0.475$					
Intercept	-0.993	-9.445	7.609	9,000	0.817
BIO01	-0.221	-1.170	0.693	10,089	0.629
BIO04	0.126	-0.904	1.258	9,000	0.815
BIO07	-0.329	-1.858	1.265	9,000	0.688
BIO13	-0.047	-0.442	0.325	9,000	0.803
BIO15	0.860	0.198	1.515	9,000	**0.010**
Body size	-0.030	-0.707	0.658	9,000	0.921
PC2; $H^2 = 0.371$					
Intercept	3.750	-6.223	13.216	10,53	0.447
BIO01	0.778	-0.299	1.863	9,310	0.162
BIO04	-1.134	-2.341	0.094	9,441	0.061[!]
BIO07	0.959	-0.802	2.644	9,000	0.278
BIO13	-0.327	-0.740	0.123	9,955	0.134
BIO15	-0.751	-1.500	-0.040	9,000	**0.048**
Body size	0.523	-0.226	1.276	9,000	0.170
PC3; $H^2 = 0.255$					
Intercept	2.830	-6.910	13.510	9,000	0.581
BIO01	-0.127	-1.341	0.970	9,000	0.831
BIO04	-0.303	-1.471	0.916	9,000	0.615
BIO07	0.455	-1.272	2.176	9,372	0.592
BIO13	-0.072	-0.508	0.374	9,289	0.737
BIO15	-0.176	-0.940	0.553	8,955	0.637
Body size	0.052	-0.751	0.858	9,000	0.894

860 Bold values indicate significance below 0.05, [!] indicates $p < 0.10$, H^2 is akin to phylogenetic

861 signal.

862

863

864

865

866 **Table 3** Results of PGLMMs predicting hair hue (RG ratio values) within the *Propithecus* genus

Variable	Mean Est.	Lower CI	Upper CI	ESS	P MCMC
PC1; $H^2 = 0.632$					
Intercept	7.664	-5.813	21.243	8,635	0.268
BIO01	-0.341	-1.656	0.811	9,000	0.584
BIO04	-0.567	-2.530	1.366	8,581	0.565
BIO07	0.751	-1.599	3.290	8,631	0.548
BIO13	0.004	-0.612	0.607	8,699	0.984
BIO15	-0.969	-2.021	0.057	8,524	0.069[!]
Body size	-0.083	-1.063	0.831	9,375	0.857
PC2; $H^2 = 0.513$					
Intercept	1.773	-8.206	11.490	8,358	0.728
BIO01	1.434	0.448	2.381	9,322	**0.006**
BIO04	-1.220	-2.587	0.153	8,042	0.076[!]
BIO07	1.154	-0.598	2.923	9,000	0.187
BIO13	-0.450	-0.907	-0.004	9,000	**0.045**
BIO15	-1.089	-1.862	-0.314	9,000	**0.006**
Body size	0.806	0.047	1.531	8,829	**0.037**
PC3; $H^2 = 0.227$					
Intercept	3.296	-0.121	1.789	9,395	0.639
BIO01	-0.429	-2.065	1.199	9,000	0.596
BIO04	-0.155	-1.744	2.085	9,492	0.903
BIO07	-0.753	-3.283	1.704	9,765	0.545
BIO13	-0.008	-0.643	-0.637	9,000	0.975
BIO15	0.001	-1.241	1.213	9,325	1.000
Body size	-0.148	-1.166	1.471	9,000	0.812

867 Bold values indicate significance below 0.05, [!] indicates $p < 0.10$, H^2 is akin to phylogenetic

868 signal.

869

870

871

872

873

874

875
876
877

878 **Table 4** Results of PGLMMs predicting hair and follicle density across all Indriidae taxa

Variable	Mean Est.	Lower CI	Upper CI	ESS	P MCMC
PC1; $H^2 = 0.222$					
Intercept	-6.478	-22.987	18.456	9,456	0.401
BIO01	-0.036	-1.368	1.366	9,000	0.961
BIO04	0.770	-0.673	2.228	9,000	0.278
BIO07	-1.093	-3.262	1.047	9,434	0.314
BIO13	0.523	-0.085	1.190	9,000	0.101
BIO15	1.232	0.185	2.255	9,290	**0.020**
Body size	-0.275	-1.326	0.770	9,339	0.597
PC2; $H^2 = 0.217$					
Intercept	0.256	-15.042	16.829	9,000	0.981
BIO01	0.175	-1.238	1.587	9,000	0.812
BIO04	0.150	-1.334	1.643	9,000	0.835
BIO07	-0.990	-3.299	1.243	9,000	0.375
BIO13	0.110	-0.523	0.806	9,000	0.736
BIO15	0.518	-0.550	1.585	9,765	0.331
Body size	-0.161	-1.266	0.922	8,309	0.760
PC3; $H^2 = 0.330$					
Intercept	10.259	-0.399	20.576	9,000	0.057[1]
BIO01	-0.259	-1.175	0.700	9,000	0.602
BIO04	0.071	-0.953	1.056	9,307	0.876
BIO07	-0.129	-1.643	1.413	9,000	0.853
BIO13	-0.337	-0.772	0.081	9,000	0.123
BIO15	0.438	-0.276	1.164	9,908	0.228
Body size	-1.265	-2.012	-0.514	9,000	**0.002**

879 Bold values indicate significance below 0.05, [1] indicates $p < 0.10$, H^2 is akin to phylogenetic signal.

880

881

882 **Table 5** Summary of ANOVA examining hair and follicle density variation across distinct body

883 regions for Indriidae

	DF	Sum Sq.	Mean Sq.	F value	P value
Hair density					
Body Region	4	1458536	364634	5.808	**< 0.0005**
Residuals	60	3766879	62781		
Follicle density					
Body Region	4	108592	27148	1.524	0.207
Residuals	60	1068659	17811		

884
885
886
887
888
889
890
891
892
893
894
895
896
897
898
899

Table 6 Results of PGLMMs predicting hair and follicle density within the *Propithecus* genus

Variable	Mean Est.	Lower CI	Upper CI	ESS	P MCMC
PC1; $H^2 = 0.256$					
Intercept	16.640	-6.426	39.799	9,000	0.142
BIO01	-1.256	-3.056	0.696	8,178	0.180
BIO04	-1.333	-3.506	0.890	8,746	0.234
BIO07	2.437	-1.147	5.812	9,286	0.176
BIO13	-0.485	-1.359	0.364	9,000	0.259
BIO15	-1.673	-3.105	-0.200	9,423	**0.028**
Body size	-0.220	-2.195	1.495	9,000	0.802
PC2; $H^2 = 0.190$					
Intercept	9.252	-17.259	37.827	9,000	0.494
BIO01	1.437	-0.749	3.688	9,000	0.192
BIO04	0.351	-2.135	2.597	9,000	0.760
BIO07	-0.042	-3.693	3.627	9,571	0.988
BIO13	-0.090	-1.141	0.898	9,356	0.862
BIO15	-0.508	-2.082	1.157	9,000	0.530
Body size	-1.632	-3.695	0.666	9,000	0.134
PC3; $H^2 = 0.279$					
Intercept	-12.391	-31.523	5.691	9,000	0.186
BIO01	0.766	-0.815	2.345	9,000	0.330
BIO04	1.090	-0.802	2.988	9,000	0.224
BIO07	-1.264	-4.442	1.564	9,000	0.382
BIO13	0.437	-0.282	1.117	9,000	0.219
BIO15	0.309	-0.864	1.559	9,000	0.606
Body size	0.738	-0.698	2.194	9,000	0.310

Bold values indicate significance below 0.05, [1] indicates $p < 0.10$, H^2 is akin to phylogenetic signal.

919 **Table 7** Summary of linear models examining pelage coloration against difference in opsin peak
920 spectral sensitivity, using hue (PC1) scores of individuals across a subset of 10 sampling
921 locations

	Estimate	**Std. Error**	**T value**	**P value**
PC1				
[Intercept]	-1.529	1.611	-0.949	0.374
Difference in Spectral Sensitivity	-0.234	0.089	-2.630	**0.034**
Number of Opsin Alleles	2.635	1.501	1.746	0.124

922 SE: 1.05 on 7 degrees of freedom; R^2= 0.516, F = 5.801 on 2 and 7 degrees of freedom; p = 0.033. Bold values
923 indicate significance below 0.05.

924
925